Energy Flow and Bond Dissociation in the Collision between Vibrationally Excited Toluene and HBr[†]

Sang Kwon Lee and Jongbaik Ree[*]

Department of Chemistry Education, Chonnam National University, Kwangju 500-757, Korea. [*]E-mail: jbree@chonnam.ac.kr
Received October 19, 2011, Accepted December 16, 2011

Molecules vibrationally excited to near their dissociation threshold can undergo both bond dissociation and vibrational relaxation, processes which play an important role in reaction dynamics.[1-5] Recent studies show that when the excited molecule is a large organic molecule, the average amount of energy transfer per collision is not very large.[4-9] The average energy transfer per collision between the highly vibrationally excited benzene and a noble gas atom is known to be about 30 cm^{-1}, which is much smaller than benzene derivatives such as hexafluorobenzene or other hydrocarbons such as toluene and azulene.[3,10-13] For example, in the case of toluene + Ar, the amount of energy transfer is about −200 cm^{-1}.[12] An important characteristic of vibrational relaxation in a large molecule is intramolecular energy flow, which plays a key role in bond dissociation. Among such large molecules, toluene is a particularly attractive molecule for studying collision-induced intramolecular energy flow and bond dissociation because of the presence of both methyl and ring C-H bonds, presenting an intriguing competition among them. In elucidating this competition, it is particularly important to understand the direction of intramolecular energy flow in the interaction zone, i.e., from the ring C-H to the methyl C-H or the reverse.

The purpose of this paper is to study the collision-induced dynamics of highly vibrationally excited toluene interacting with HBr using quasiclassical trajectory calculations. Using the results obtained in the calculations, we discuss the relaxation of the excited CH vibration, and the time evolution of collision-induced intramolecular energy flow from the highly excited CH vibration. Finally, we elucidate the nature and mechanism of competition between methyl C-H mode and ring C-H mode in transferring energy to or from the incident molecule.

Interaction Model and Numerical Procedures

The present work follows the interaction model and numerical pocedure, which have already been reported in Ref. 9. Briefly, we recapitulate the essential aspects of the interaction of HBr with toluene in this section. The model for the toluene-HBr interaction and vibrational coordinates
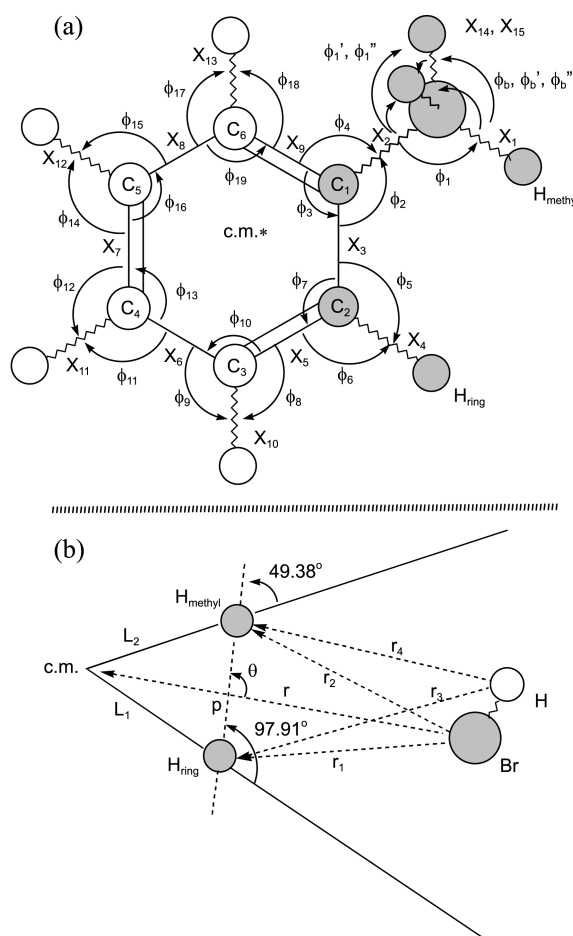

Figure 1. Collision model. (a) The stretching and bending coordinates of vibrations included in the model. All carbon atoms and ring H atoms are coplanar and the vibrational modes are numbered clockwise. The star denotes the center-of-mass (cm) of toluene. For convenience we identify each vibration by its displacement (e.g., x_1 for $x_{e1} + x_1$). (b) The relative coordinate between HBr and the cm of toluene (r), the Br-to-H$_{ring}$ distance (r_1), the Br-to-H$_{methyl}$ distance (r_2), H-to-H$_{ring}$ distance (r_3) and H-to-H$_{methyl}$ distance (r_4) are shown.

of toluene are defined in Figure 1, where all carbon atoms, the ring hydrogen atoms and the incident molecule are assumed to be coplanar. In Figure 1(a), we define all 39 intramolecular coordinates of the planar ring needed to be included in the present study. In Figure 1(b), we define the

---

interaction coordinates between the C-H$_{methyl}$ bond and the adjacent C-H$_{ring}$ bond of a non-rotating toluene with the incident HBr molecule. For the intermolecular interaction, we take $D = 414k_B$, the Lennard-Jones (LJ) parameter for the well depth for the collision pairs calculated by the usual combining rule,[14] where k_B is the Boltzmann constant, and $a = 0.272$ Å.[15] For the ith stretch, we use $b_i = (2D_i/\mu_i\omega_i^2)^{1/2}$, where $D_i = D_{o,i} + \frac{1}{2} \omega_{ei}$, to determine the exponential range parameters listed in Table 1 of Ref. 8. The potential and spectroscopic constants for the HBr are $D_{0,HBr}^0 = 3.758$ eV and $\omega_{HBr}/2\pi c = 2649$ cm^{-1}.[16] The exponential range parameter b_{HBr} is 0.553 Å determined from the relation $b_{HBr} = (2D_{HBr}/\mu_{HBr}\omega_{HBr}^2)^{1/2}$. The equilibrium distance of HBr is $d_{HBr} = 1.414$ Å.[17] In the coupling terms, $Y_i = x_i$ or ϕ_i and the coupling constants K_{ij} are taken from Xie and Boggs' ab initio calculations.[17] In our calculations, we have already shown that the interaction near $\theta = 77°$ plays the dominant role in promoting energy loss or C-H bond dissociation through inter- or intra-molecular energy transfer.[5] Thus, in all collision systems considered here, the incident atom approaches the center of mass (c.m.) of toluene in the $\theta = 77°$ direction, where the C-H$_{methyl}$-HBr and C-H$_{ring}$-HBr interactions are very close to each other and where energy transfer is most efficient.[5]
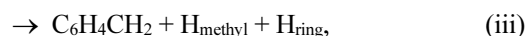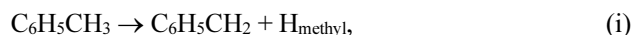
We solve the equations of motion for the relative motion, 15 stretches and 24 bends of toluene, and HBr vibration using the DIVPAG double-precision routine of the IMSL library[18,19] to describe the time evolution of bond distances, bond angles, and vibrational energies, as well as the relative coordinate for the model system. We sample 40,000 trajectories for each run at 300 K, where the sampling includes determining collision energies (E) chosen from the Maxwell distribution. In studying the E dependence of energy transfer and bond dissociation, we carry out the same sampling except that E is now fixed at a specified value. The initial conditions for solving the equations of motion for the relative motion and the displacements and phases for the vibrational motions in the interaction zone are given in Ref. 5. We vary the initial vibrational energies of the C-H$_{ring}$ and C-H$_{methyl}$ bonds (i.e, $i = 1$ and 4) systematically, while maintaining the rest of the vibrational motions in the ground state. Each vibrational phase is a random number $\delta_i = 2\pi s_i$ with flat distribution of s_i in the interval (0,1). The initial separation between the c.m.'s of toluene and HBr is set as 15 Å, and trajectories are terminated when the separation reaches 50 Å after they passed through the closest distance of approach. The integration was performed with a stepsize of 0.169 fs, which is one-tenth the period of the largest frequency, the ring CH vibration, and is small enough to ensure energy conservation to at least five significant figures along a trajectory. We have also confirmed that the numerical procedure allows the trajectories to be successfully backintegrated.

Results and Discussion

In Figure 2, we show the dependence of energy loss on the total vibrational energy content E_T for $\theta = 77°$ at 300 K. The smallest value of E_T considered in this figure is 12,454 cm^{-1} or 1.544 eV, which corresponds to the vibrational energies of C-H$_{methyl}$ and C-H$_{ring}$ being 2274 cm^{-1} (0.282 eV) and 10,180 cm^{-1} (1.262 eV), respectively. That is, both bonds are 3.5 eV below the dissociation threshold of each bond. At this total vibrational energy content, the energy loss is 1570 cm^{-1} or 0.1948 eV. Below $E_T = 30,000$ cm^{-1}, the magnitude of energy loss is nearly constant. As shown in Figure 2, for example, when E_T is raised from 12,454 cm^{-1} to 30,000 cm^{-1}, $-\langle\Delta E\rangle$ varies from 1570 cm^{-1} to 1700 cm^{-1}. As the total energy content continues to increase, however, $-\langle\Delta E\rangle$ decreases gradually, finally falling to 229 cm^{-1} at $E_T = 67,290$ cm^{-1}, which corresponds to each bond's vibrational energy only 0.1 eV below the dissociation threshold. In Figure 2, we also show the energy losses for Toluene-HCl and Toluene-HF systems. The energy loss is significantly different from the Toluene-HCl[20] and Toluene-HF[9] systems. In the latter cases the energy loss shows the maximum in the range discussed. That is, it increases slowly with increasing total vibrational energy content between 20,000 and 45,000 cm^{-1}, and above the energy content of 45,000 cm^{-1} energy loss decreases. Even though the former is significantly different from the latter, the overall slow variations of $-\langle\Delta E\rangle$ with increasing E_T are similar and this trend has been known to be the general behavior for the relaxation of toluene by rare gases and diatomic molecules such as N$_2$ in experimental and theoretical studies.[4,15,21]

We now discuss the collision-induced dissociation of highly excited toluene molecules. The possible dissociation pathways of toluene in the present system are

$$C_6H_5CH_3 \rightarrow C_6H_5CH_2 + H_{methyl}, \tag{i}$$

$$\rightarrow C_6H_4CH_3 + H_{ring}, \tag{ii}$$

$$\rightarrow C_6H_4CH_2 + H_{methyl} + H_{ring}, \tag{iii}$$

where Reactions (i) and (ii) produce a radical while Reaction (iii), requiring a greater energy, produces a diradical.

We plot the dissociation probabilities at 300 K for $\theta = 77°$ in Figure 3. Here we take as before both C-H bonds have their initial vibrational energies which are below their respective dissociation threshold by the same amount. When each of them is 1.0 eV or 8,065 cm^{-1} below the threshold, the total vibrational energy content is 52,780 cm^{-1} above the
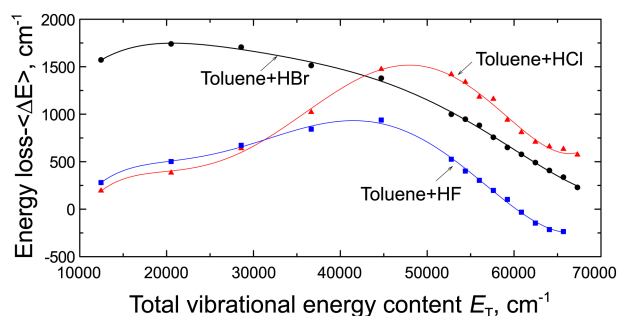

Figure 2. Energy loss against the total vibrational energy content E_T for $\theta = 77°$ at $T = 300$ K.

zero point energy with 30,340 cm^{-1} in C-H$_{ring}$ and 22,440 cm^{-1} in C-H$_{methyl}$, the dissociation probabilities are $P_{C\text{-}Hmethyl}$ = 0.0129 and $P_{C\text{-}Hring}$ = 0.0024. Here dissociation probabilities are very small because a large amount of energy has to be deposited in one of the bonds. We note that the ensemble-averaged energy loss by toluene for E_T = 52,780 cm^{-1} is 999 cm^{-1} or 0.1239 eV as shown in Figure 2. Since the C-H$_{methyl}$ (or C-H$_{ring}$) bond is 8,065 cm^{-1} below its dissociation threshold, this bond has to gain at least 8,065 cm^{-1} from C-H$_{ring}$ (or C-H$_{methyl}$) through intramolecular energy redistribution to dissociate.

As shown in Figure 3, $P_{C\text{-}Hmethyl}$ is always greater than $P_{C\text{-}Hring}$ for the total vibrational energy content chosen such that both bonds are below their respective dissociation threshold by the same amount of energy at 300 K. When the total energy content is increased from 52,780 cm^{-1} toward the dissociation threshold, the probabilities rise very rapidly. When E_T is as high as 67,294 cm^{-1}, which corresponds to each bond's vibrational energy only 0.1 eV below the dissociation threshold, the dissociation probabilities are now $P_{C\text{-}Hmethyl}$ = 0.0440 and $P_{C\text{-}Hring}$ = 0.0113. Such large values indicate that the vibrational motions of a highly excited molecule can be readily perturbed by the incident molecule and the molecule need only a small amount of energy to dissociate. Also, in such a highly excited molecule, both C-H bonds can dissociate even though the probability for simultaneous dissociation would be very small. In fact, the probability of simultaneous dissociation of C-H$_{methyl}$ and C-H$_{ring}$ is 0.0002, which shows that the majority of dissociative events involve breaking only one C-H bond.

In Figure 4, we show the dependence of the dissociation probabilities of C-H bonds on the collision energy for E_T = 60,850 cm^{-1}, which corresponds to each bond's vibrational energy only 0.5 eV below the dissociation threshold. As shown in Figure 4, the dissociation probability of C-H$_{methyl}$

bond is always larger than that of C-H$_{ring}$. This result is consistent with the result presented in Figure 3 at thermal energies. At E = 2 eV, $P_{C\text{-}Hmethyl}$ is as large as 0.254, whereas $P_{C\text{-}Hring}$ is only 0.031. At such high collision energies, where HBr approaches very close to toluene, the incident molecule can maintain a near-collinear alignment with C-H$_{methyl}$ for efficient perturbation. Such alignment is not possible for C-H$_{ring}$ at close range. Furthermore, at such high collision energies, when energy transfer between toluene and HBr is large, energy flow to the inner region of the molecule can be important. In particular, the energy initially deposited in the C-H$_{ring}$ vibration will readily flow to this region, when the molecule is strongly perturbed. A low probability of dissociation for C-H$_{ring}$ seen in Figure 4 at high collision energies is due to the initial energy propagating through the C-C bonds and then finally accumulating in the inner region of the molecule, rather than in the C-H$_{methyl}$.

As shown in Figures 5(a) and 5(a'), whereas the lifetime distribution for the C-H$_{ring}$ bond dissociation shows an induction period of ≈ 0.1 ps, that for C-H$_{methyl}$ bond dissociation shows no induction period. The disparity in the two induction periods reveals a subtle aspect of the collision dynamics in which two different energy transfer mechanisms operate, which can be discussed by comparing the results of a representative reactive collision (Figures 5(b) and 5(c)) for the C-H$_{methyl}$ dissociation and those (Figs. 5(b') and 5(c')) for the C-H$_{ring}$ dissociation. The time evolution of the C-H$_{methyl}$ bond trajectory is shown in Figure 5(b), where the large amplitude motion of the excited bond suddenly diverges as HBr approaches. The time evolution of the C-H$_{methyl}$ vibrational energy shows a sharp energy jump, the bond gaining nearly 0.53 eV (see Figure 5(c)), which exceeds the amount needed to dissociate. The energy jump occurs in three steps over a short time period of 100fs, which is approximately one period of the excited C-H$_{methyl}$ bond
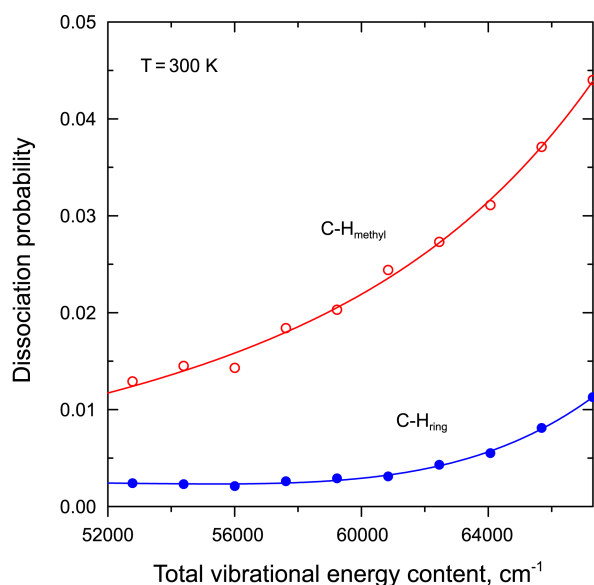

Figure 3. Dissociation probabilities of C-H$_{methyl}$ and C-H$_{ring}$ bonds against the total vibrational energy content E_T for θ = 77° at T = 300 K.

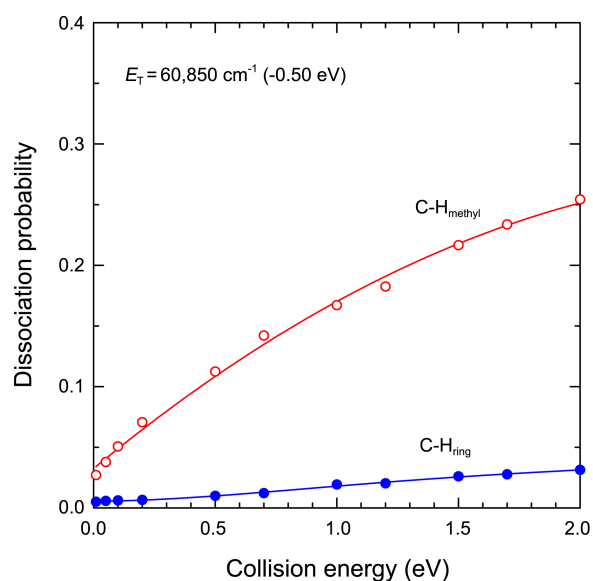**Figure 4.** Dissociation probabilities of C-H$_{methyl}$ and C-H$_{ring}$ bonds against the collision energy for the total vibrational energy content E_T = 60,850 cm^{-1} and θ = 77°.
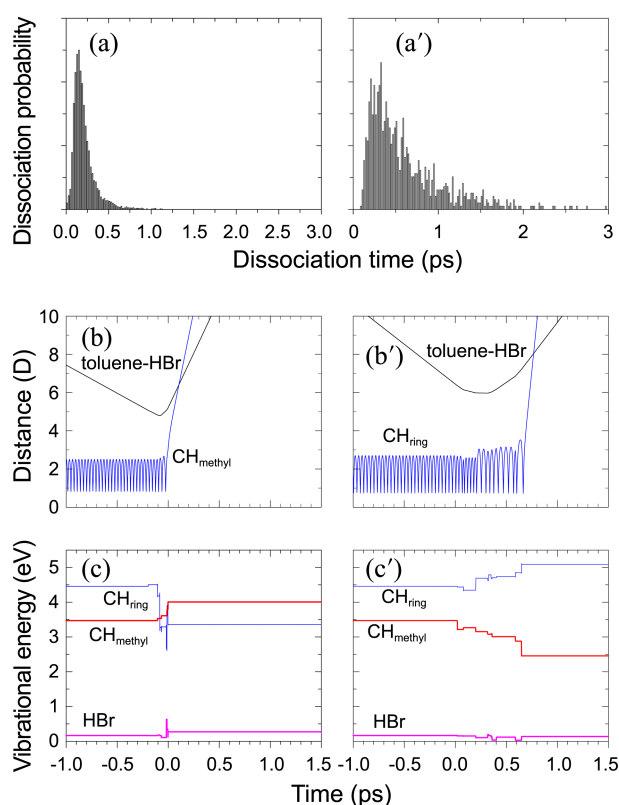
Figure 5. Dependence of the C-H dissociation probability on the dissociation time τ for (a) the C-H$_{methyl}$ bond and (a') C-H$_{ring}$ bond for $E_T = 60{,}850$ cm^{-1}. Time evolution of the collision trajectory and C-H bond trajectory for: (b) C-H$_{methyl}$ and (b') C-H$_{ring}$. The same scale is used for both figures. Time evolution of the C-H$_{methyl}$, C-H$_{ring}$ and HBr vibrational energies for (c) C-H$_{methyl}$ dissociation trajectory and (c') C-H$_{ring}$ dissociation trajectory. The time scale is the same for (b), (b'), (c), and (c').

stretching. From a dramatic change in the vibrational energies of C-H$_{methyl}$ and C-H$_{ring}$ before and after collision shown in Figure 5(b), we notice that the energy jump is mainly caused by V→V energy transfer from C-H$_{ring}$.

For the trajectory representing the C-H$_{ring}$ dissociation shown in Figure 5(b'), the C-H$_{ring}$ bond trajectory takes nearly 0.8 ps before diverging. During this period, energy flows from C-H$_{methyl}$ to C-H$_{ring}$, i.e., the energy imparted to H$_{methyl}$ flows to H$_{ring}$. The time scale of the energy buildup in C-H$_{ring}$ closely matches that of the energy loss in C-H$_{methyl}$, as they are linked by the energy flow path (see Figure 5(c')). For the representative trajectory depicted in Figure 5(c'), the C-H$_{methyl}$ bond loses 0.61 eV while the C-H$_{ring}$ bond gains

0.50 eV. Therefore, the overall energy loss during this collision is 0.11 eV (≈ 887 cm^{-1}). Note that the overall energy loss ΔE for the entire ensemble of all collisions at $E_T = 60{,}842$ cm^{-1} is only 576 cm^{-1}. Once a sufficient amount of energy deposits in the C-H$_{ring}$ bond, the dissociation can occur rapidly. It is important to notice in Figure 5(c') that the activation of C-H$_{ring}$ occurs in a series of small energy transfer steps, the variation which is significantly different from the sudden two or three-step excitation behavior of the C-H$_{methyl}$ activation seen in Figure 5(c).

References

1. Smith, I. W. M. in *Gas Kinetics and Energy Transfer, Vol. 2*; Specialist Periodical Reports; Chemical Society, Burlington House: London, 1977; pp 1-57.
2. Yardley, J. T. *Introduction to Molecular Energy Transfer*; Academic: New York, 1980.
3. Clary, D. C.; Gilbert, R. G.; Bernshtein, V.; Oref, I. *Faraday Discuss.* **1995**, *102*, 423.
4. Wright, S. M. A.; Sims, I. R.; Smith, I. W. M. *J. Phys. Chem. A* **2000**, *104*, 10347.
5. Ree, J.; Kim, Y. H.; Shin, H. K. *J. Chem. Phys.* **2002**, *116*, 4858.
6. Shin, H. K. *J. Phys. Chem. A* **2000**, *104*, 6699.
7. Nilsson, D.; Nordholm, S. *J. Chem. Phys.* **2002**, *116*, 7040.
8. Ree, J.; Kim, Y. H.; Shin, H. K. *Chem. Phys. Lett.* **2004**, *394*, 250.
9. (a) Ree, J.; Chang, K. S.; Kim, Y. H.; Shin, H. K. *Bull. Kor. Chem. Soc.* **2003**, *24*, 1223. (b) Ree, J.; Kim, Y. H.; Shin, H. K. *Bull. Kor. Chem. Soc.* **2005**, *26*, 1269. (c) Ree, J.; Kim, S. H.; Lee, T. H.; Kim, Y. H. *Bull. Kor. Chem. Soc.* **2006**, *27*, 495.
10. Yerram, M. L.; Brenner, J. D.; King, K. D.; Barker, J. R. *J. Phys. Chem.* **1990**, *94*, 6341.
11. Damm, M.; Hippler, H.; Olschewski, H. A.; Troe, J.; Willner, J. *Z. Phys. Chem.* **1990**, *166*, 129.
12. Toselli, B. M.; Brenner, J. D.; Yerram, M. L.; Chin, W. E.; King, K. D.; Barker, J. R. *J. Chem. Phys.* **1991**, *95*, 176.
13. Damm, M.; Deckert, F.; Hippler, H.; Troe, J. *J. Phys. Chem.* **1991**, *95*, 2005.
14. Hirschfelder, J. O.; Curtiss, C. F.; Bird, R. B. *Molecular Theory of Gases and Liquids*; Wiley: New York, 1967; see p 168 for the combining laws, pp 1110-1112 and 1212-1214 for D and σ.
15. Lim, K. F. *J. Chem. Phys.* **1994**, *100*, 7385.
16. Huber, K. P.; Herzberg, G. *Constants of Diatomic Molecules*; Van Nostrand Reinhold: New York, 1979.
17. Xie, Y.; Boggs, J. E. *J. Comp. Chem.* **1986**, *7*, 158.
18. Gear, C. W. *Numerical Initial Value Problems in Ordinary Differential Equations*; Prentice-Hall: New York, 1971.
19. MATH/LIBRARY, *Fortran Subroutines for Mathematical Applications*; IMSL: Houston, 1989; p 640.
20. Kook, M.; Ree, J.; Lee, T. H. *J. Sci. Educ. (Chonnam National University)* **2004**, *28*, 195.
21. Shi, J.; Barker, J. R. *J. Chem. Phys.* **1988**, *88*, 6219.